frontiers | Frontiers in Control Engineering

TYPE Original Research
PUBLISHED 10 January 2023
DOI 10.3389/fcteg.2022.1083419

Check for updates

OPEN ACCESS

EDITED BY
Tito Luís Maia Santos,
Federal University of Bahia, Brazil

REVIEWED BY
Andrzej Pawlowski,
University of Brescia, Italy
Damir Vrancic,
Institut Jožef Stefan (IJS), Slovenia

*CORRESPONDENCE
Hu Xingqi,
✉ 18601260651@163.com

SPECIALTY SECTION
This article was submitted to Control and Automation Systems, a section of the journal
Frontiers in Control Engineering

RECEIVED 29 October 2022
ACCEPTED 12 December 2022
PUBLISHED 10 January 2023

CITATION
Xingqi H, Guolian H and Wen T (2023), Tuning of *PIDD*^{2} controllers for oscillatory systems with time delays.
Front. Control. Eng. 3:1083419.
doi: 10.3389/fcteg.2022.1083419

COPYRIGHT
© 2023 Xingqi, Guolian and Wen. This is an open-access article distributed under the terms of the Creative Commons Attribution License (CC BY). The use, distribution or reproduction in other forums is permitted, provided the original author(s) and the copyright owner(s) are credited and that the original publication in this journal is cited, in accordance with accepted academic practice. No use, distribution or reproduction is permitted which does not comply with these terms.

Tuning of *PIDD*^{2} controllers for oscillatory systems with time delays

Hu Xingqi[1]*, Hou Guolian[1] and Tan Wen[2]

[1]School of Control and Computer Engineering, North China Electric Power University, Beijing, China, [2]School of Electrical and Control Engineering, North China University of Technology, Beijing, China

Proportional–integral–derivative (PID) control is a durable control technology that has been widely applied in the process control industry. However, PID controllers cannot achieve satisfactory performance for oscillatory systems with long time delays; thus, high-order controllers like the proportional–integral–double derivative (*PIDD*^{2}) can be adopted to enhance the control performance. In this paper, we propose a tuning formula for the *PIDD*^{2} controller for oscillatory systems with time delays and its practical implementation *via* an observer bandwidth-based state-space *PIDD*^{2}. Simulation results show that the state-space *PIDD*^{2} controller tuned from the proposed formula trades-off among robustness, time domain performance, and measurement noise attenuation and can arrive at a better control effect than PID for oscillatory systems.

KEYWORDS

oscillatory systems, internal model control, parameter tuning, robustness, time domain performance, measurement noise, PID plus second-order controller

1 Introduction

Proportional–integral–derivative (PID) control is a durable control technology that has been widely applied in the process control industry (Kim and Lee, 2021). The principal reason is its relatively simple structure, which can be easily implemented, understood, and maintained in practical industry production processes. PID is so wildly used in process control system applications, and it is one of the important factors in the development of the industry (Borase et al., 2021). Hence, most studies in the field of process control have only focused on PID control, which includes intelligent PID (Chan et al., 2007; Gundes and Ozguler, 2007), fuzzy PID (Tzafestas and Papanikolopoulos, 1990; Jin et al., 2017), optimal PID (Halikias and Zolotas, 1999; Chao et al., 2019; Memon and Shao, 2020; Memon and Shao, 2021), adaptive PID control (Radke and Isermannt, 1987; Pan et al., 2007), and fractional-order PID (Zhao et al., 2005; Chevalier et al., 2019).

It is well-known that the oscillatory dynamics of the process have various features, and parameter tuning is complicated and difficult. To facilitate research, the oscillatory dynamics of the process can be modeled as the standard second-order process with a dead-time (SOPDT) model. Up to now, research on the tuning of the SOPDT system has been mostly restricted to PID. Weng et al. (1997) derived the tuning formula of the PID controller based on the gain and phase margin for the underdamped oscillatory system. The user-specified gain and phase margins can be adaptively achieved, but the trade-off optimization between stability and tracking performance is not designed. Wang et al. (1999) proposed a PID controller parameter tuning method based on the closed-loop pole assignment strategy of the root locus for the oscillatory system; the parameter design process is more complicated. Huang et al. (2000) proposed an inverse-based synthesis PID controller for the oscillatory system and analyzed its robustness by the gain and phase margins. However, the effect of noise was not considered. Basilio and Matos (2002) designed the PID controller for the underdamping system, but the controlled plant did not account for dead time. Oliveira and Vrančić (2012) addressed the problem of decreasing the overshoot by switching controllers for underdamped second-order systems, which is not convenient for practical engineering applications.

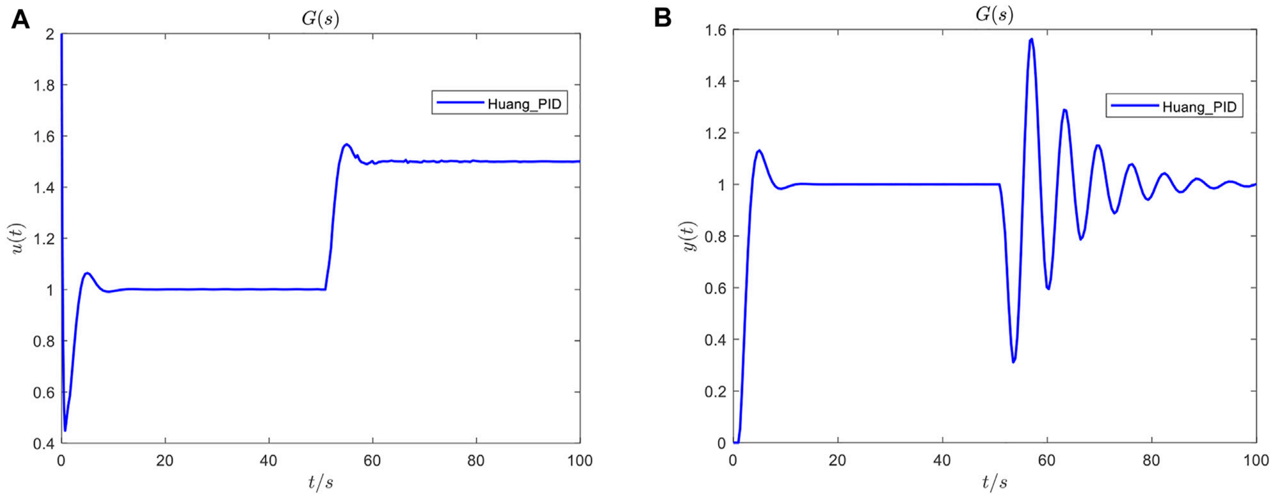

FIGURE 1
Dynamic response of the SOPDT model under PID: **(A)** controller output responses and **(B)** system output responses.

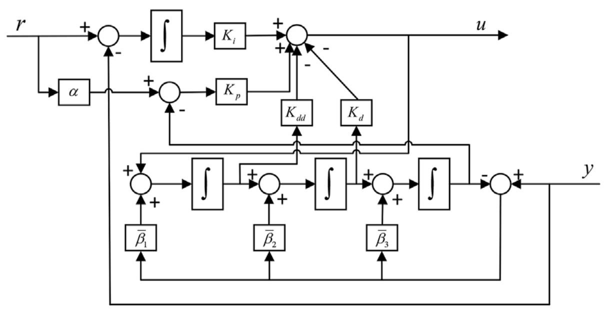

FIGURE 2
Block diagram of the state-space $PIDD^2$ controller.

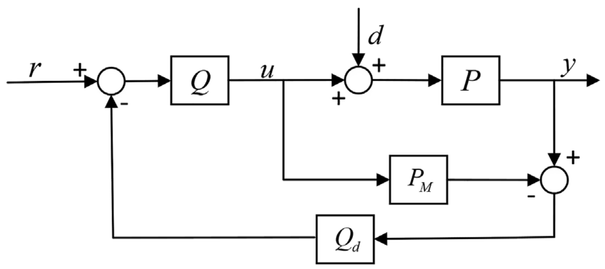

FIGURE 3
Block diagram of TDF-IMC.

Kurokawa et al. (2020) proposed an optimal trade-off PID control system for a SOPDT system, which does not consider the impact of measurement noise. The aforementioned literature reports are devoted to the study of the controller from the perspective of the frequency domain. Although some research has been carried out on PID controllers, it is still unclear whether or not PID can effectively handle oscillatory process uncertainties like disturbance and measurement noise. Furthermore, it may be necessary to manually adjust the PID controller for the step response of the oscillatory process through trial and error, which may inevitably result in inaccuracies. More importantly, it is difficult for the conventional PID controller to guarantee the stability of the oscillatory process with a time delay. The scenario is quite different from the step response of the non-oscillatory plant, where numerous well-known formulas exist (Lee et al., 1998; Skogestad and Grimholt, 2012; Garpinger et al., 2014). Therefore, it would be desirable if there are tuning criteria for the oscillatory plant with time delays to improve the performance of systems.

As an example, consider the following oscillatory system with a time delay ($G(s)$):

$$G(s) = \frac{1}{s^2 + 0.2s + 1} e^{-s}. \tag{1}$$

The dynamic response of SOPDT under the conventional PID (Huang et al., 2000) is shown in Figure 1 when a unit step reference signal (the amplitude is 1) is inserted at $t = 0s$ and an input disturbance signal (the amplitude is 5) is inserted at $t = 50s$. Controller parameters are $K_p = 0.1; K_i = 0.5; K_d = 0.5;$ from Figure 1, we can see that although the tracking response of PID is acceptable, the rejection–disturbance response is still oscillatory, which is undesired.

To improve the performance of conventional PID, a new conventional controller named the proportional–integral–double derivative ($PIDD^2$) is widely used (kalyan and Suresh, 2021; Koley et al., 2020; Mokeddem and Mirjalili, 2020; Simanenkov et al., 2017; Sonkar and Rahi, 2016). The $PIDD^2$ controller is robust and capable of controlling the automatic voltage regulator under load frequency control system uncertainties (Mohanty, 2018; Chatterjee et al., 2019). So far, there are only some literature studies about parameter tuning for $PIDD^2$, e.g., CSA–$PIDD^2$ (Koley et al., 2020), hFPA-PS–$PIDD^2$ (Mohanty, 2020), GWO–$PIDD^2$ (Kalyan, 2021), and Fuzzy–$PIDD^2$ (Farooq et al., 2021). However, the $PIDD^2$ controller is not discussed for oscillatory systems. In reality, oscillatory systems are not subject to any special $PIDD^2$ tuning rules. To tune oscillatory SOPDT systems, this paper proposes the tuning formula of $PIDD^2$.

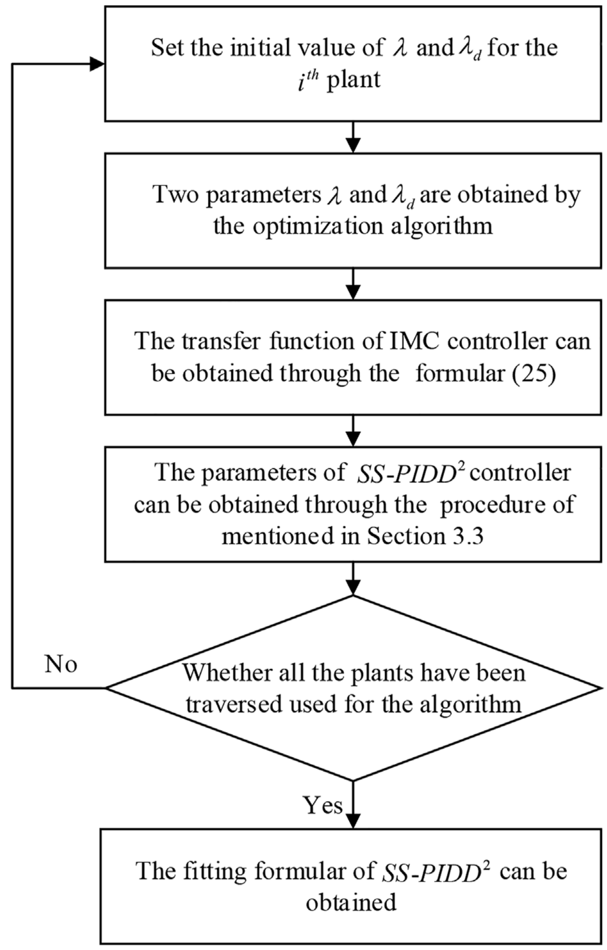

FIGURE 4
Flow chart of the derivation of the tuning formula.

For practical implementation issues, we will investigate a state-space $PIDD^2$ control structure. The state-space $PIDD^2$ controller estimates the derivative of the controlled plant output *via* an observer. The second-order differentiation is utilized to reduce impacts of fluctuation of the disturbance. The state-space $PIDD^2$ controller retains the plant-independent property of the traditional PID and overcomes some of its disadvantages. For oscillatory systems with time delays, a tuning formula based on the state-space $PIDD^2$ controller is proposed first, and then, the parameters of $PIDD^2$ are obtained *via* the well-known internal model control (IMC) framework for oscillatory systems. The proposed tuning formula is tested for a wide variety of simulation examples and the load frequency control system. It is shown that the state-space $PIDD^2$ controller outperforms the traditional PID in oscillatory systems. The state-space $PIDD^2$ controller trades-off among disturbance rejection performance, robustness, and attenuation of the measurement noise.

The rest of the paper consists of four parts. In Section 2, $PIDD^2$ and its state-space implementation is introduced; tuning of the state-space $PIDD^2$ controller based on IMC for the SOPDT system is introduced in Section 3; Section 4 presents simulation and analysis results. Finally, conclusions are given in Section 5.

2 $PIDD^2$ and its state-space implementation

A PID controller has been frequently utilized in the industry due to its simplicity and efficiency. The $PIDD^2$ controller has been used to enhance the performance of the conventional PID controller. The structure of $PIDD^2$ is similar to the conventional PID, in addition to the extra second-order derivative gain. An ideal $PIDD^2$ controller has the following transfer function form:

$$C_{PIDD}(s) = K_p + \frac{K_i}{s} + K_d s + K_{dd} s^2, \tag{2}$$

where K_p, K_i, K_d, and K_{dd} are the proportional variable, integral variable, derivative gain, and double derivative gain, respectively. $PIDD^2$ control can be written as a state-feedback control law, given as follows:

$$\begin{aligned} u(t) &= K_{dd}(\ddot{r}(t) - \ddot{y}(t)) + K_d(\dot{r}(t) - \dot{y}(t)) \\ &\quad + K_p(r(t) - y(t)) + K_i\int_0^t (r(\tau) - y(\tau))d\tau \\ &=: \bar{K}_o(\bar{r}(t) - x(t)). \end{aligned} \tag{3}$$

Here, $y(t)$ is the controlled variable, $u(t)$ is the manipulated variable, and $r(t)$ is the reference signal.

$$\bar{r}(t) = \left[\begin{array}{cccc} \ddot{r}(t) & \dot{r}(t) & r(t) & \int_0^t r(\tau)d\tau \end{array}\right]^T. \tag{4}$$

The state vector is as follows:

$$x(t) = \left[\begin{array}{cccc} \ddot{y}(t) & \dot{y}(t) & y(t) & \int_0^t y(\tau)d\tau \end{array}\right]^T. \tag{5}$$

The state-feedback gain is as follows:

$$\bar{K}_o = \left[\begin{array}{cccc} K_{dd} & K_d & K_p & K_i \end{array}\right]. \tag{6}$$

The state vector $x(t)$ (5) contains the derivative of $y(t)$, so it cannot be measured directly. An observer can be adopted to estimate it. Consider the following triple integral model:

$$\dddot{y}(t) = u(t). \tag{7}$$

Let

$$x_1 = \ddot{y}, \quad x_2 = \dot{y}, \quad x_3 = y. \tag{8}$$

Then, Eq. 7 can be written in the following state-space form:

$$\begin{cases} \begin{bmatrix} \dot{x}_1 \\ \dot{x}_2 \\ \dot{x}_3 \end{bmatrix} = \bar{A}_o \begin{bmatrix} x_1 \\ x_2 \\ x_3 \end{bmatrix} + \bar{B}_o u, \\ y = \bar{C}_o \begin{bmatrix} x_1 \\ x_2 \\ x_3 \end{bmatrix}, \end{cases} \tag{9}$$

where

$$\bar{A}_o = \begin{bmatrix} 0 & 0 & 0 \\ 1 & 0 & 0 \\ 0 & 1 & 0 \end{bmatrix}, \bar{B}_o = \begin{bmatrix} 1 \\ 0 \\ 0 \end{bmatrix}, \bar{C}_o = \left[\begin{array}{ccc} 0 & 0 & 1 \end{array}\right]. \tag{10}$$

Thus, the following Luenberger observer can be used to estimate $[\ddot{y} \quad \dot{y} \quad y]^T$.

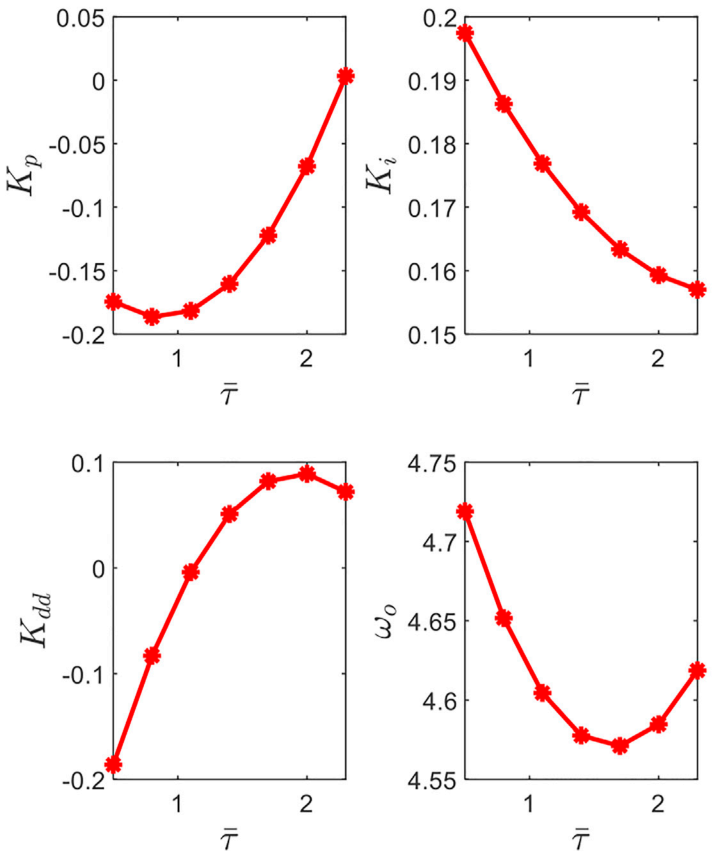

FIGURE 5
Fitting curves of parameters of SS-***PIDD***^{2}.

$$\begin{bmatrix} \dot{\bar{x}}_1 \\ \dot{\bar{x}}_2 \\ \dot{\bar{x}}_3 \end{bmatrix} = (\bar{A}_o - \bar{L}\bar{C}_o)\begin{bmatrix} \bar{x}_1 \\ \bar{x}_2 \\ \bar{x}_3 \end{bmatrix} + \bar{B}_o u + \bar{L}y, \tag{11}$$

where $\bar{L}$ is the observer gain, which is given as follows:

$$\bar{L} = \left[\bar{\beta}_1 \;\; \bar{\beta}_2 \;\; \bar{\beta}_3\right]^T. \tag{12}$$

If $\bar{L}$ is chosen such that $\bar{A}_o - \bar{L}\bar{C}_o$ is asymptotically stable, then $\widehat{\bar{x}}_1 \to \ddot{y}$, $\widehat{\bar{x}}_2 \to \dot{y}$, and $\widehat{\bar{x}}_3 \to y$. Furthermore, $\int_0^t y(\tau)d\tau$ can be computed using another state $\widehat{\bar{x}}_4$, where

$$\dot{\bar{x}}_4 = \bar{x}_3 = y. \tag{13}$$

By combining Eq. 11 and Eq. 13, we have an estimation of the state vector of Eq. 5 with the following observer:

$$\dot{\bar{x}} = (\bar{A}_e - \bar{L}_o\bar{C}_e)\bar{x} + \bar{B}_e u + \bar{L}_o y, \tag{14}$$

where $\bar{x} = [\,\bar{x}_1 \;\; \bar{x}_2 \;\; \bar{x}_3 \;\; \bar{x}_4\,]^T$ and

$$\bar{A}_e = \begin{bmatrix} 0 & 0 & 0 & 0 \\ 1 & 0 & 0 & 0 \\ 0 & 1 & 0 & 0 \\ 0 & 0 & 1 & 0 \end{bmatrix}, \bar{B}_e = \begin{bmatrix} 1 \\ 0 \\ 0 \\ 0 \end{bmatrix}, \bar{C}_e = [\,0 \;\; 0 \;\; 1 \;\; 0\,]. \tag{15}$$

$\bar{L}_o$ is the observer gain vector shown as follows:

$$\bar{L}_o = \left[\bar{\beta}_1 \;\; \bar{\beta}_2 \;\; \bar{\beta}_3 \;\; 1\right]^T. \tag{16}$$

When $\bar{L}_o$ is chosen properly, $\bar{A}_e - \bar{L}_o\bar{C}_e$ is asymptotically stable, and

$$\bar{x}_1(t) \to \ddot{y}(t), \bar{x}_2(t) \to \dot{y}(t), \bar{x}_3(t) \to y(t), \bar{x}_4(t) \to \int_0^t y(\tau)d\tau. \tag{17}$$

Hence, the third-order state-space PID is the implementation of $PIDD^2$, and an ideal $PIDD^2$ controller can be approximated with the following third-order state-space PID (SS-$PIDD^2$) controller:

$$\begin{cases} \dot{\bar{x}}_1 = (\bar{A}_e - \bar{L}_o\bar{C}_e)\bar{x} + \bar{B}_e u + \bar{L}_o y, \\ u = \bar{K}_o(\bar{r} - \bar{x}). \end{cases} \tag{18}$$

So the feedback controller from y to u is as follows:

$$K_c(s) = \bar{K}_o\left(sI - \bar{A}_e + \bar{B}_e\bar{K}_o + \bar{L}_o\bar{C}_e\right)^{-1}\bar{L}_o$$
$$= \frac{\left(K_{dd}\bar{\beta}_1 + K_d\bar{\beta}_2 + K_p\bar{\beta}_3 + K_i\right)s^3 + \left(K_d\bar{\beta}_1 + K_p\bar{\beta}_2 + K_i\bar{\beta}_3\right)s^2 + \left(K_p\bar{\beta}_1 + K_i\bar{\beta}_2\right)s + K_i\bar{\beta}_1}{s\left[s^3 + (K_{dd} + \bar{\beta}_3)s^2 + (K_{dd}\bar{\beta}_3 + K_d + \bar{\beta}_2)s + \bar{\beta}_1 + K_{dd}\bar{\beta}_2 + K_d\bar{\beta}_3 + K_p\right]}. \tag{19}$$

$\bar{K}_o$ is the controller gain vector, as shown in Eq. 6.

Figure 2 shows the structural block diagram of the third-order state-space PID (SS-$PIDD^2$). α is the set-point weight, which is used to reduce the overshoot. By default, $\alpha = 1$.

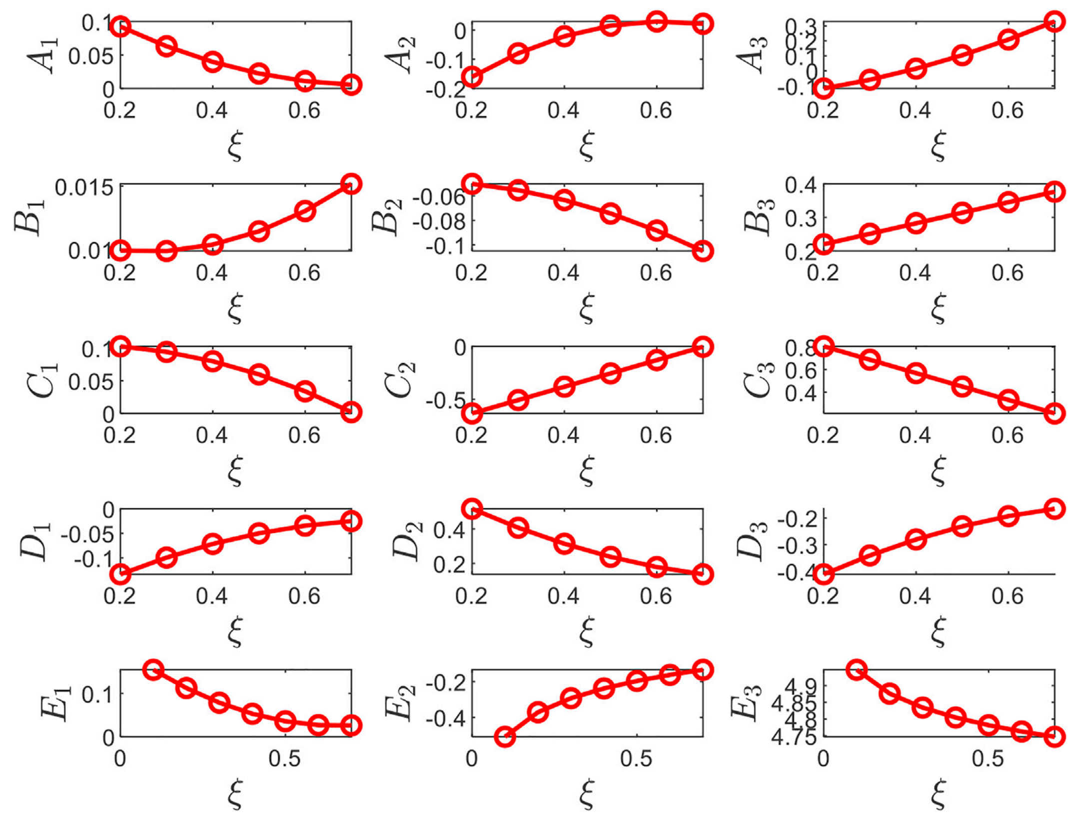

FIGURE 6
Fitting curves of K_p, K_i, K_d, K_{dd}, ω_o, and ξ.

3 Tuning of the state-space *PIDD*^{2} controller based on IMC for the SOPDT system

The dynamics of the oscillatory SOPDT system is relatively complicated, and the controller parameter design process faces severe challenges. In general, the low-order controller often neglects the higher-order dynamics of oscillatory systems. Thus, the result of the control effect is not accurate (Wang et al., 2021). The well-known internal model control has the advantage of using one or two tuning parameters to achieve good control performance to model inaccuracies (Shamsuzzoha and Lee, 2007, p.). Therefore, in this section, we will discuss in detail how the parameters of the SS-*PIDD*^{2} controller are obtained using IMC.

3.1 Description of the internal model control (IMC)

Figure 3 shows the structural block diagram of the two-degree-of-freedom IMC (TDF-IMC) controller. $P(s)$ is the plant to be controlled, and $P_M(s)$ is the plant model; $Q(s)$ is the set-point tracking controller, and $Q_d(s)$ is the disturbance rejection controller.

We can divide the design process of the TDF-IMC controller into the following steps (Tan and Fu, 2015):

1) Factor the plant model $P_M(s)$ into two parts:

$$P_M(s) = P_{M_+}(s)P_{M_-}(s), \tag{20}$$

where $P_{M_+}(s)$ is the portion of the model inverted (minimum-phase) and $P_{M_-}(s)$ is the portion of the model not inverted (non-minimum-phase).

2) Design the set-point tracking controller $Q(s)$ as follows:

$$Q(s) = P_{M_+}^{-1}(s)f(s), \tag{21}$$

where $f(s)$ is a low-pass filter and its expression is given as follows:

$$f(s) = \frac{1}{(\lambda s+1)^n}. \tag{22}$$

Here, λ is the filter parameter, and n is the relative degree of $P_{M_+}(s)$.

3) The disturbance rejection controller $Q_d(s)$ is designed as follows:

$$Q_d(s) = \frac{\alpha_m s^m + \cdots + \alpha_1 s + 1}{(\lambda_d s+1)^{r_d}}, \tag{23}$$

where m is the number of poles of $P_M(s)$ such that $Q_d(s)$ needs to cancel the disturbance rejection filter $\frac{1}{(\lambda_d s+1)^{r_d}}$ with order $r_d \geq m$, and λ_d is a tuning parameter for obtaining a better disturbance-rejecting performance. The poles $p_1 \cdots p_m$ of $P_M(s)$ can be canceled by the zeros $\alpha_1 \cdots \alpha_m$ of $Q_d(s)$, i.e., $\alpha_1 \cdots \alpha_m$ should satisfy the following:

$$(1 - P_M(s)Q(s)Q_d(s))|_{s=p_1\cdots p_m} = 0. \tag{24}$$

The corresponding transfer function of the IMC controller is as follows:

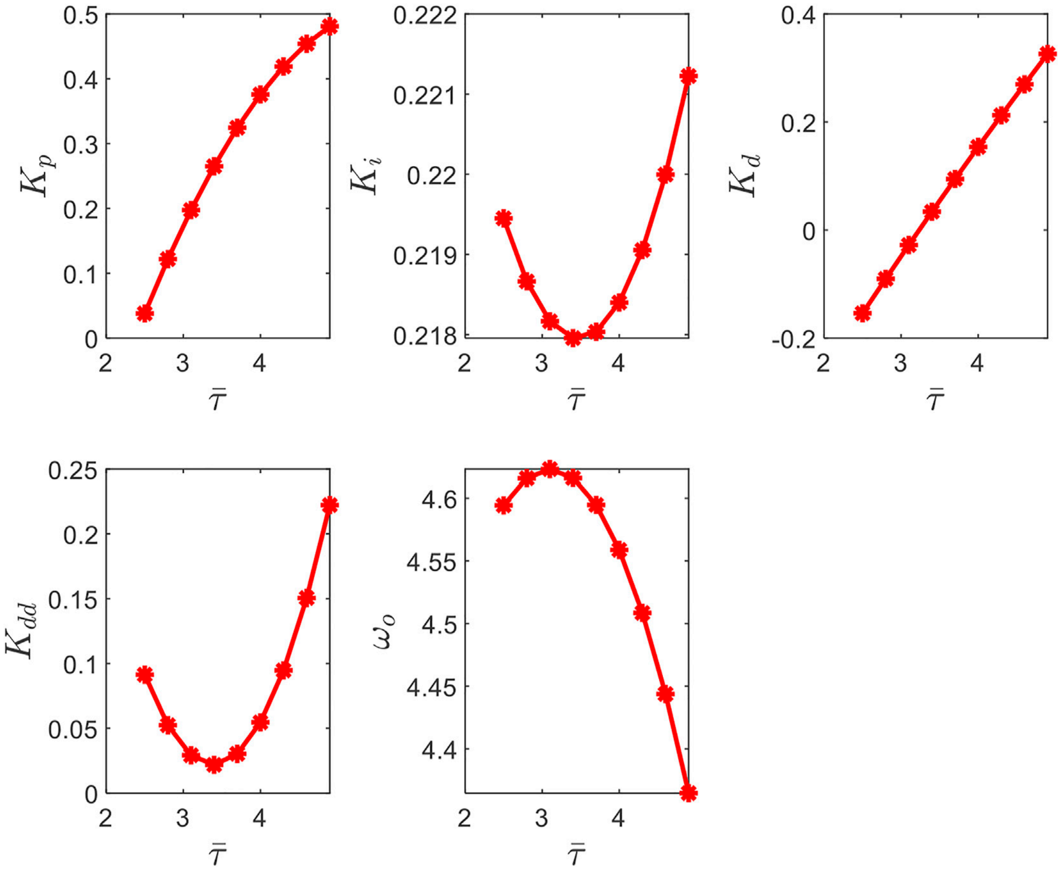

FIGURE 7
Fitting curves of parameters of SS-***PIDD***^{2}.

$$K_{IMC}(s) = \frac{Q(s)Q_d(s)}{1 - P_M(s)Q(s)Q_d(s)}. \tag{25}$$

3.2 The IMC controller design for the SOPDT system

By designing the IMC controller, we can get the controller gain of SS-$PIDD^2$. So consider the general form of SOPDT systems as follows:

$$P_M(s) = \frac{k}{T^2s^2 + 2T\xi s + 1}e^{-\tau s} \tag{26}$$

The controllers $Q(s)$ and $Q_d(s)$ for Eq. 26 are as follows:

$$Q(s) = \frac{T^2s^2 + 2T\xi s + 1}{k(\lambda s + 1)^2} \tag{27}$$

$$Q_d(s) = \frac{\alpha_2 s^2 + \alpha_1 s + 1}{(\lambda_d s + 1)^3} \tag{28}$$

Here, the order of the disturbance rejection filter r_d is chosen as 3, and α_1 and α_2 meet Eq. 24.

From the aforementioned derivation, the final form of Eq. 25 is given as follows:

$$K_{IMC}(s) = \frac{1}{k}\frac{(T^2s^2 + 2T\xi s + 1)(\alpha_2 s^2 + \alpha_1 s + 1)}{(\lambda s + 1)^2(\lambda_d s + 1)^3 - (\alpha_2 s^2 + \alpha_1 s + 1)e^{-\tau s}}. \tag{29}$$

From the aforementioned analysis, we can cancel the roots of $T^2s^2 + 2T\xi s + 1$. To obtain a finite-dimensional controller, we take the first-order Pade approximation technique (Horn et al., 1996; Shamsuzzoha and Lee, 2008) to approximate the pure delay.

$$e^{-\tau s} = \frac{1 - \frac{\tau}{2}s}{1 + \frac{\tau}{2}s}. \tag{30}$$

Then, the simplified form of Eq. 29 becomes

$$K_{IMC}(s) = \frac{1}{k}\frac{\left(1 + \frac{\tau}{2}s\right)(\alpha_2 s^2 + \alpha_1 s + 1)}{s(a_3 s^3 + a_2 s^2 + a_1 s + 1)} = \frac{p_3 s^3 + p_2 s^2 + p_1 s + p_0}{s(q_3 s^3 + q_2 s^2 + q_1 s + q_0)}, \tag{31}$$

where the expression of $p_0, \cdots, p_3$ and $q_0, \cdots, q_3$ can be obtained as follows:

$$p_0 = 1,\quad p_1 = \frac{\tau}{2} + \alpha_1,\quad p_2 = \frac{\tau}{2}\alpha_1 + \alpha_2,\quad p_3 = \frac{\tau}{2}\alpha_2, \tag{32}$$

$$q_0 = 2\lambda + 3\lambda_d + \alpha_1 + \tau,$$
$$q_1 = \frac{\alpha_1}{2}\tau - \alpha_2 + 6\lambda\lambda_d + (2\lambda + 3\lambda_d)\frac{\tau}{2} + \lambda^2 + 3\lambda_d^2 - 2T\xi q_0,$$

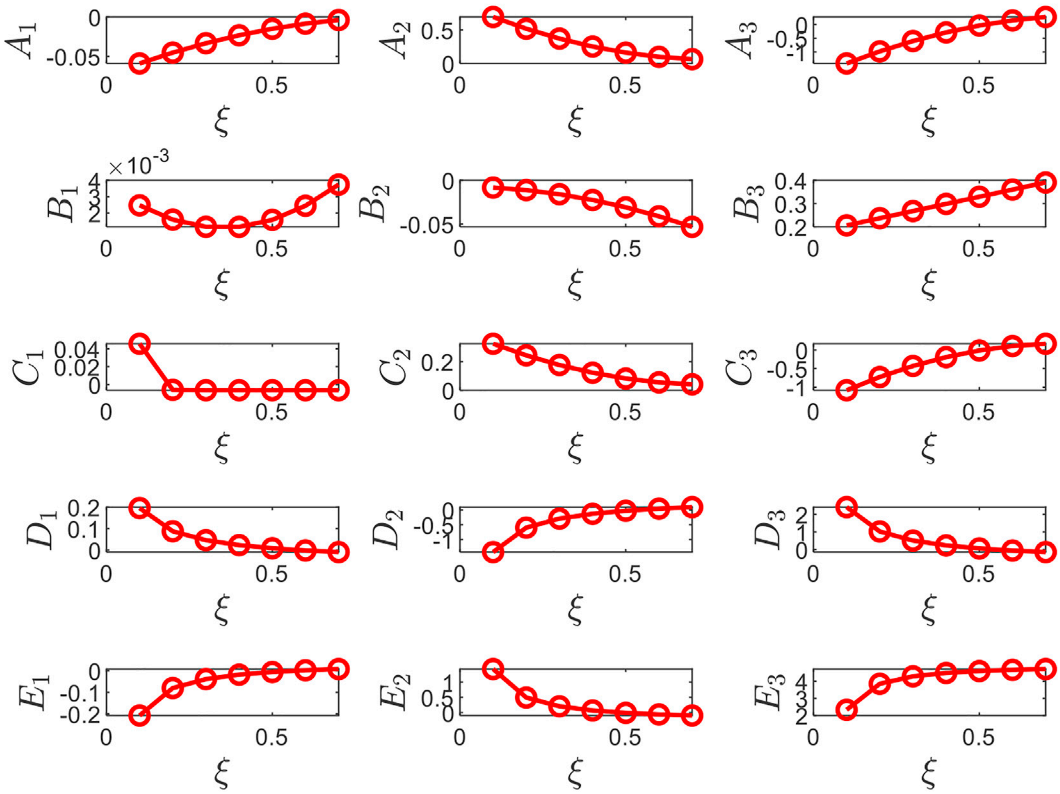

FIGURE 8
Fitting curves of K_p, K_i, K_d, K_{dd}, ω_o, and ξ.

$$q_2 = \frac{\frac{(3\lambda^2\lambda_d^2 + 2\lambda\lambda_d^3)^2}{2} + \lambda^2\lambda_d^3 - 2T\xi q_3}{T^2}, q_3 = \frac{\lambda^2\lambda_d^3}{2T^2}\tau. \tag{33}$$

3.3 Specific approximate processes with the state-space $PIDD^2$

This subsection focuses on how to attain the parameters of SS-$PIDD^2$ through IMC. For simplicity, the observer gain $\bar{L}_o$ in Eq. 16 can be tuned *via* the bandwidth idea (Gao, 2003), i.e., the poles of $\bar{A}_e - \bar{L}_o\bar{C}_e$ in Eq. 14 are placed at the same location $-\bar{\omega}_o$, and then,

$$\bar{\beta}_1 = \bar{\omega}_o{}^3,\quad \bar{\beta}_2 = 3\bar{\omega}_o{}^2,\quad \bar{\beta}_3 = 3\bar{\omega}_o. \tag{34}$$

According to the aforementioned Eq. 19, the transfer function form of SS-$PIDD^2$ is as follows:

$$\begin{aligned} K_c(s) &= \bar{K}_o\left(sI - \bar{A}_e + \bar{B}_e\bar{K}_o + \bar{L}_o\bar{C}_e\right)^{-1}\bar{L}_o \\ &= \frac{c_3s^3 + c_2s^2 + c_1s + c_0}{s\left(e_3s^3 + e_2s^2 + e_1s + e_0\right)}, \end{aligned} \tag{35}$$

where

$$\begin{bmatrix} c_3 \\ c_2 \\ c_1 \\ c_0 \end{bmatrix} = \begin{bmatrix} \bar{\beta}_1 & \bar{\beta}_2 & \bar{\beta}_3 & 1 \\ 0 & \bar{\beta}_1 & \bar{\beta}_2 & \bar{\beta}_3 \\ 0 & 0 & \bar{\beta}_1 & \bar{\beta}_2 \\ 0 & 0 & 0 & \bar{\beta}_1 \end{bmatrix} \begin{bmatrix} K_{dd} \\ K_d \\ K_p \\ K_i \end{bmatrix}, \tag{36}$$

$$\begin{bmatrix} e_3 \\ e_2 \\ e_1 \\ e_0 \end{bmatrix} = \begin{bmatrix} 1 & 0 & 0 & 0 \\ \bar{\beta}_3 & 1 & 0 & 0 \\ \bar{\beta}_2 & \bar{\beta}_3 & 1 & 0 \\ \bar{\beta}_1 & \bar{\beta}_2 & \bar{\beta}_3 & 1 \end{bmatrix} \begin{bmatrix} 1 \\ K_{dd} \\ K_d \\ K_p \end{bmatrix}. \tag{37}$$

To make the SS-$PIDD^2$ controller achieve the same control performance as the IMC controller, suppose Eq. 31 and 35 have the same zeros, i.e.,

$$\begin{bmatrix} c_3 \\ c_2 \\ c_1 \\ c_0 \end{bmatrix} = \alpha \begin{bmatrix} p_3 \\ p_2 \\ p_1 \\ p_0 \end{bmatrix}, \tag{38}$$

where α is an optional constant. According to Eq. 36, we have the following:

$$\begin{bmatrix} c_3 \\ c_2 \\ c_1 \\ c_0 \end{bmatrix} = \begin{bmatrix} \bar{\beta}_1 & \bar{\beta}_2 & \bar{\beta}_3 & 1 \\ 0 & \bar{\beta}_1 & \bar{\beta}_2 & \bar{\beta}_3 \\ 0 & 0 & \bar{\beta}_1 & \bar{\beta}_2 \\ 0 & 0 & 0 & \bar{\beta}_1 \end{bmatrix} \begin{bmatrix} K_{dd} \\ K_d \\ K_p \\ K_i \end{bmatrix} = \alpha \begin{bmatrix} p_3 \\ p_2 \\ p_1 \\ p_0 \end{bmatrix}. \tag{39}$$

Thus, the controller gain of SS-$PIDD^2$ can be obtained as follows:

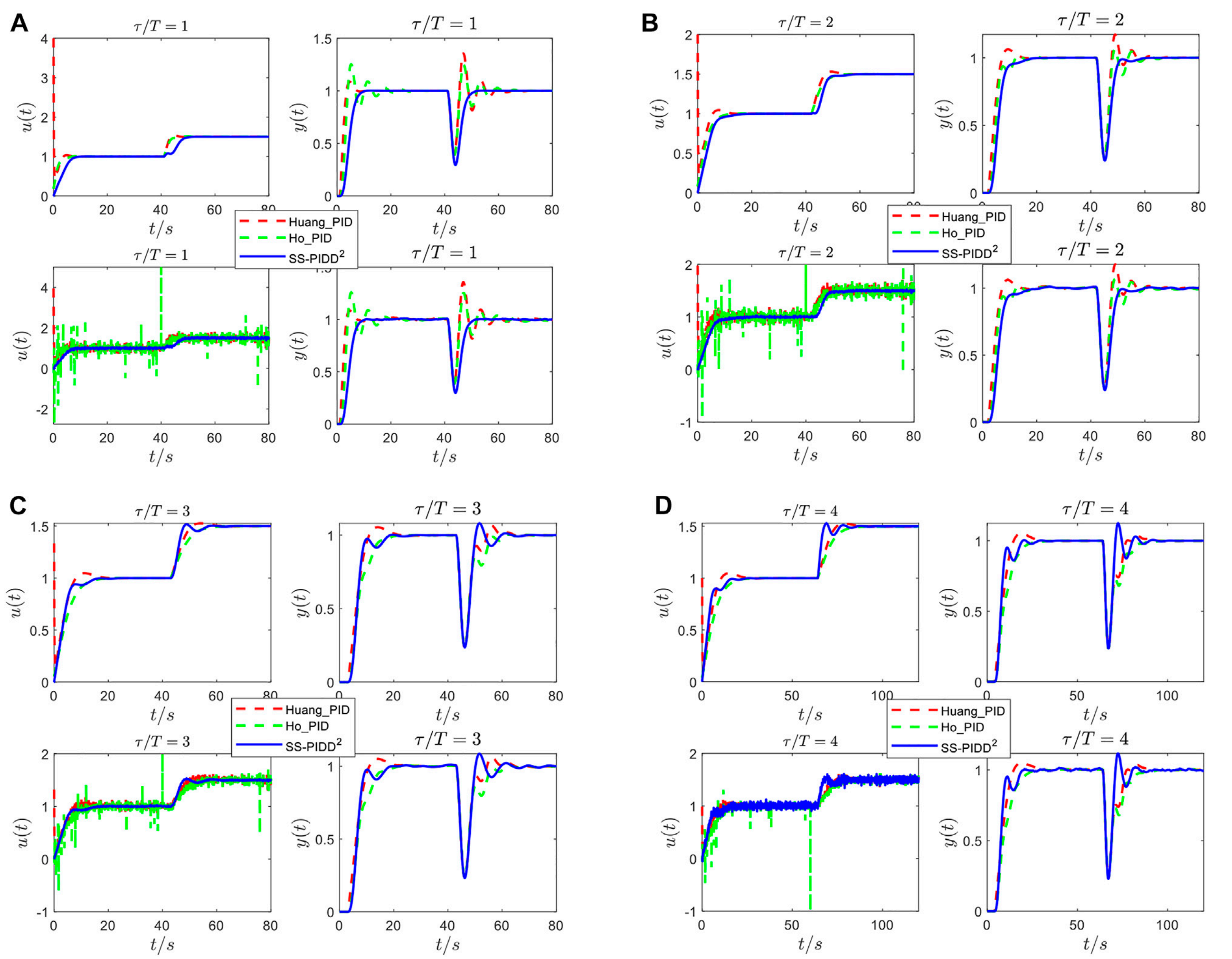

FIGURE 9
Responses of the SOPDT system with ξ = .2 under different controllers: controller output responses without noise [the top left of **(A–D)**]; system output responses without noise [the top right of **(A–D)**]; controller output responses with noise [the bottom left of **(A–D)**]; **(B)** system output responses with noise [the bottom right of **(A–D)**].

$$\begin{bmatrix}K_{dd}\\K_d\\K_p\\K_i\end{bmatrix} = \alpha \begin{bmatrix}\bar\beta_1&\bar\beta_2&\bar\beta_3&1\\0&\bar\beta_1&\bar\beta_2&\bar\beta_3\\0&0&\bar\beta_1&\bar\beta_2\\0&0&0&\bar\beta_1\end{bmatrix}^{-1}\begin{bmatrix}p_3\\p_2\\p_1\\p_0\end{bmatrix}$$

$$= \alpha \begin{bmatrix}\frac{1}{\bar\beta_1}&-\frac{\bar\beta_2}{\bar\beta_1{}^2}&\frac{\bar\beta_2{}^2-\bar\beta_1\bar\beta_3}{\bar\beta_1{}^3}&\frac{2\bar\beta_1\bar\beta_2\bar\beta_3-\bar\beta_2{}^3-\bar\beta_1{}^2}{\bar\beta_1{}^4}\\0&\frac{1}{\bar\beta_1}&-\frac{\bar\beta_2}{\bar\beta_1{}^2}&\frac{\bar\beta_2{}^2-\bar\beta_1\bar\beta_3}{\bar\beta_1{}^3}\\0&0&\frac{1}{\bar\beta_1}&-\frac{\bar\beta_2}{\bar\beta_1{}^2}\\0&0&0&\frac{1}{\bar\beta_1}\end{bmatrix}\begin{bmatrix}p_3\\p_2\\p_1\\p_0\end{bmatrix}$$

$$\begin{aligned}&= \alpha\frac{1}{\bar\beta_1}p_3-\alpha\frac{\bar\beta_2}{\bar\beta_1{}^2}p_2+\alpha\frac{\bar\beta_2{}^2-\bar\beta_1\bar\beta_3}{\bar\beta_1{}^3}p_1+\alpha\frac{2\bar\beta_1\bar\beta_2\bar\beta_3-\bar\beta_2{}^3-\bar\beta_1{}^2}{\bar\beta_1{}^4}p_0\\&= \alpha\frac{1}{\bar\beta_1}p_2-\alpha\frac{\bar\beta_2}{\bar\beta_1{}^2}p_1+\alpha\frac{\bar\beta_2{}^2-\bar\beta_1\bar\beta_3}{\bar\beta_1{}^3}p_0\\&= \alpha\frac{1}{\bar\beta_1}p_1-\alpha\frac{\bar\beta_2}{\bar\beta_1{}^2}p_0 \quad = \frac{1}{\bar\beta_1}p_0.\end{aligned} \tag{40}$$

The final parameters of SS-$PIDD^2$ can be obtained by substituting Eqs 32 and 34 into Eq. 40. The important thing to note here is to make α as large as possible so that $\bar\omega_o$ is a positive real-number.

3.4 Tuning rules for SOPDT systems

The performance of the IMC controller is decided by the parameters λ and λ_d. Nevertheless, previous studies of the IMC have not dealt with how to obtain the appropriate value of these two parameters. In other words, there is no specific approach to choose the value of λ and λ_d. Hence, the core idea of this subsection is to get optimized values of λ and λ_d. The optimal values of λ and λ_d are those that give the minimum (integral of the time squared error) ITSE with certain robustness, and then, we can get the transfer function of the equivalent IMC controller. Thus, according to Section 3.3, we can obtain the parameters (K_p; K_i; K_d; K_{dd}; ω_o) of the SS-$PIDD^2$ controller. The specific flow chart of the derivation process is shown in Figure 4.

In the process of calculating the parameters of SS-$PIDD^2$, as mentioned in Figure 4, we notice that the parameters of the

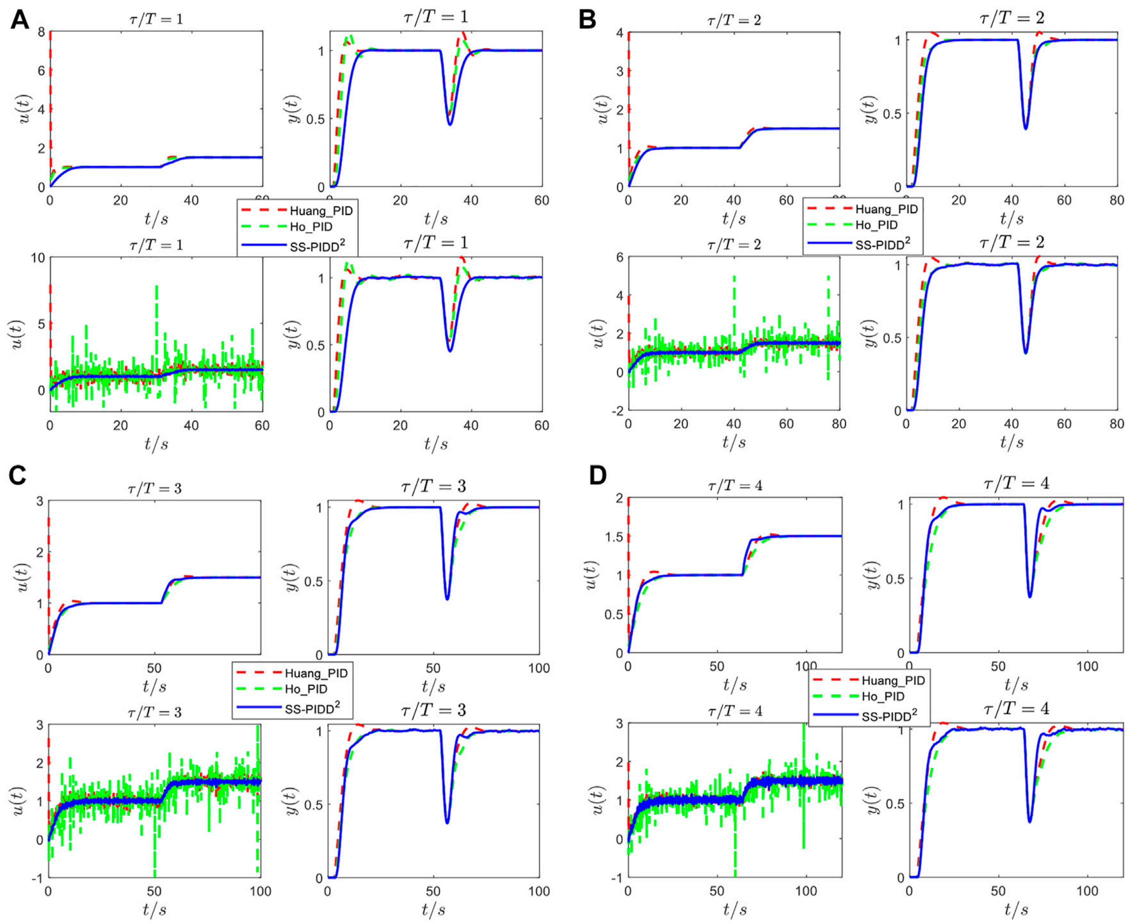

FIGURE 10
Responses of the SOPDT system with $\xi = 0.4$ under different controllers: controller output responses without noise [the top left of **(A–D)**]; system output responses without noise [the top right of **(A–D)**]; controller output responses with noise [the bottom left of **(A–D)**]; **(B)** system output responses with noise [the bottom right of **(A–D)**].

SS-$PIDD^2$ controller exhibit different properties for $\tau/T \le 2.5$ and $\tau/T > 2.5$; consequently, we set the parameters in the two cases, respectively.

To describe the detailed derivation process of the tuning formula, suppose $\tau/T \le 2.5$ and consider a normalized SOPDT system, then

$$G(s) = \frac{1}{s^2 + 2 \times 0.2 \times s + 1} e^{-\bar{\tau} s}, \tag{41}$$

where $\bar{\tau}$ varies from .5 to 2.5 with an appropriate step. A set of parameters of SS-$PIDD^2$ K_p, K_i, K_d, K_{dd}, and ω_o can be obtained through the process in Figure 4. The fitting curves of parameters of the SS-$PIDD^2$ are shown in Figure 5.

The corresponding function expressions are given in Eq. 42:

$$\begin{aligned}
\bar{K}_p &= 0.0924\bar{\tau}^2 - 0.1599\bar{\tau} - 0.1176,\\
\bar{K}_i &= 0.0099\bar{\tau}^2 - 0.0502\bar{\tau} + 0.2201,\\
\bar{K}_d &= 0.1027\bar{\tau}^2 - 0.6332\bar{\tau} + 0.8056,\\
\bar{K}_{dd} &= -0.1334\bar{\tau}^2 + 0.5169\bar{\tau} - 0.4112,\\
\bar{\omega}_o &= 0.1125\bar{\tau}^2 - 0.3707\bar{\tau} + 4.8762.
\end{aligned} \tag{42}$$

So we can rewrite Eq. 42 as follows:

$$\begin{aligned}
\bar{K}_p &= A_1\bar{\tau}^2 + A_2\bar{\tau} + A_{3,}\\
\bar{K}_i &= B_1\bar{\tau}^2 + B_2\bar{\tau} + B_3,\\
\bar{K}_d &= C_1\bar{\tau}^2 + C_2\bar{\tau} + C_3,\\
\bar{K}_{dd} &= D_1\bar{\tau}^2 + D_2\bar{\tau} + D_3,\\
\bar{\omega}_o &= E_1\bar{\tau}^2 + E_2\bar{\tau} + E_3.
\end{aligned} \tag{43}$$

When $\xi = 0.1; 0.3; 0.4; 0.5; 0.6; 0.7$, the corresponding fitting curves of $K_p, K_i, K_d, K_{dd}, \omega_o$, and ξ are obtained, as shown in Figure 6. The fitting formulae are given in Eq. 44:3

$$\begin{aligned}
A_1 &= 0.3\xi^2 - 0.4434\xi + 0.1691,\\
A_2 &= -1.102\xi^2 + 1.354\xi - 0.3866,\\
A_3 &= 0.7656\xi^2 + 0.2038\xi - 0.189,\\
B_1 &= 0.02727\xi^2 - 0.01403\xi + 0.01164,\\
B_2 &= -0.1443\xi^2 + 0.02041\xi - 0.04854,\\
B_3 &= 0.313\xi + 0.1575,\\
C_1 &= -0.2909\xi^2 + 0.06036\xi + 0.1023,\\
C_2 &= 1.258\xi - 0.8848,\\
C_3 &= -1.187\xi + 1.043,\\
D_1 &= -0.3103\xi^2 + 0.4958\xi - 0.2201,\\
D_2 &= 0.8436\xi^2 - 1.519\xi + 0.787,\\
D_3 &= -0.5418\xi^2 + 0.9786\xi - 0.5852,\\
E_1 &= 0.4148\xi^2 - 0.5456\xi + 0.205,\\
E_2 &= -3.695\xi^{-0.04876} + 3.626,\\
E_3 &= -56.83\xi^{0.00182} + 61.54,
\end{aligned} \tag{44}$$

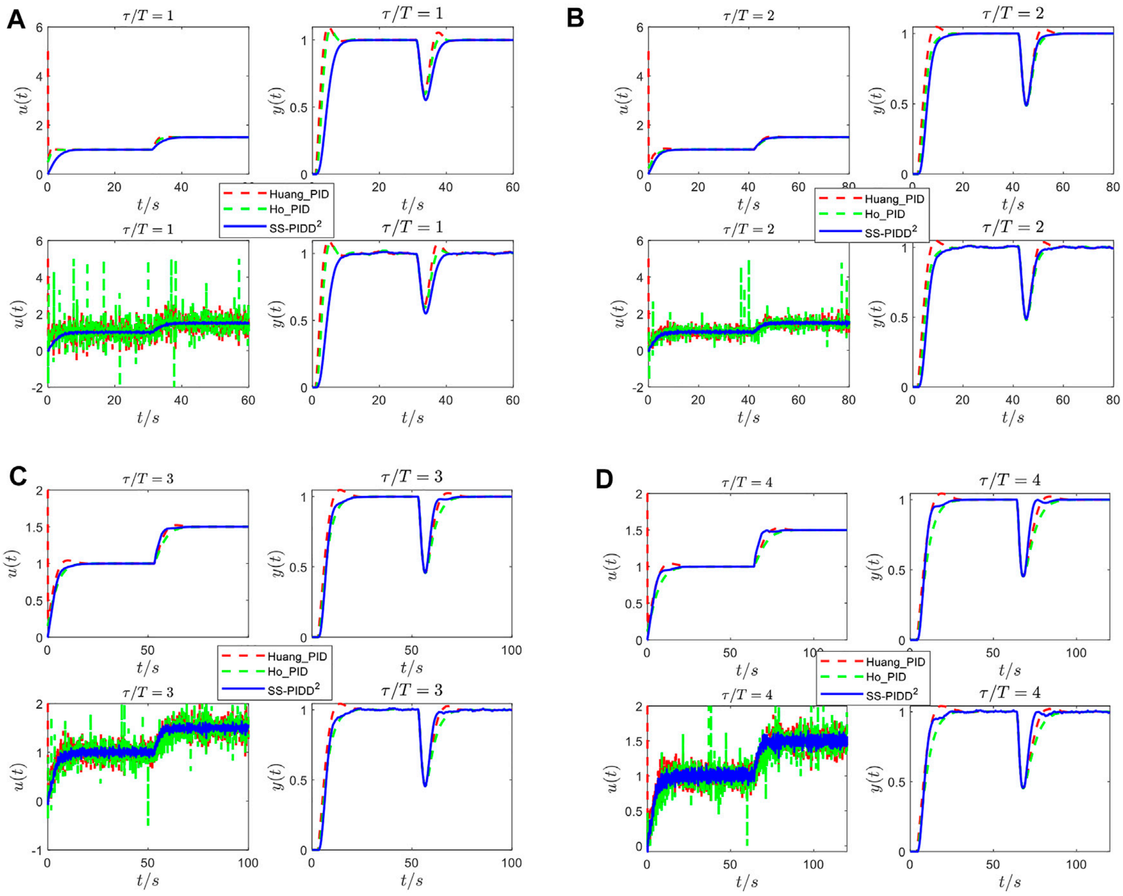

FIGURE 11
Responses of the SOPDT system with $\xi = 0.6$ under different controllers: controller output responses without noise [the top left of **(A–D)**]; system output responses without noise [the top right of **(A–D)**]; controller output responses with noise [the bottom left of **(A–D)**]; **(B)** system output responses with noise [the bottom right of **(A–D)**].

TABLE 1 Parameters of the SS-*PIDD*^{2} and PID controllers for $\xi = 0.2$.

System parameters		Method	Controller parameters				ITSE index	Robustness index	Total variation
			K_p	K_i	K_d	K_{dd}	ITSE	ε	TV
$\xi = 0.2$	$\tau/T = 1$	SS-$PIDD^2$	−0.1851	−0.1798	0.2751	−0.0276	653.5863	2.2285	7.4161
		Huang_PID	0.2	0.5	0.5		544.8031	2.5540	60.9785
		Ho_PID	0.1798	0.3840	0.3840		453.6361	2.1748	810.5307
	$\tau/T = 2$	SS-$PIDD^2$	−0.0677	0.1593	−0.0499	0.0893	992.6308	2.5074	2.8541
		Huang_PID	0.1	0.25	0.25		781.9585	2.4548	30.5162
		Ho_PID	0.0833	0.1920	0.1920		788.3334	1.9964	390.8009
	$\tau/T = 3$	SS-$PIDD^2$	0.1734	0.1701	−0.0484	0.0348	1.143e+03	2.9843	1.9509
		Huang_PID	0.0667	0.1667	0.1667		1.118e+03	2.4211	20.3436
		Ho_PID	0.0541	0.1280	0.1280		1.267e+03	2.0051	272.0857
	$\tau/T = 4$	SS-$PIDD^2$	0.3761	0.1702	0.1539	0.0540	1.503e+03	3.4939	19.4144
		Huang_PID	0.05	0.125	0.125		1.761e+03	2.4038	24.9336
		Ho_PID	0.04	0.096	0.096		2.06e+03	2.0079	328.9098

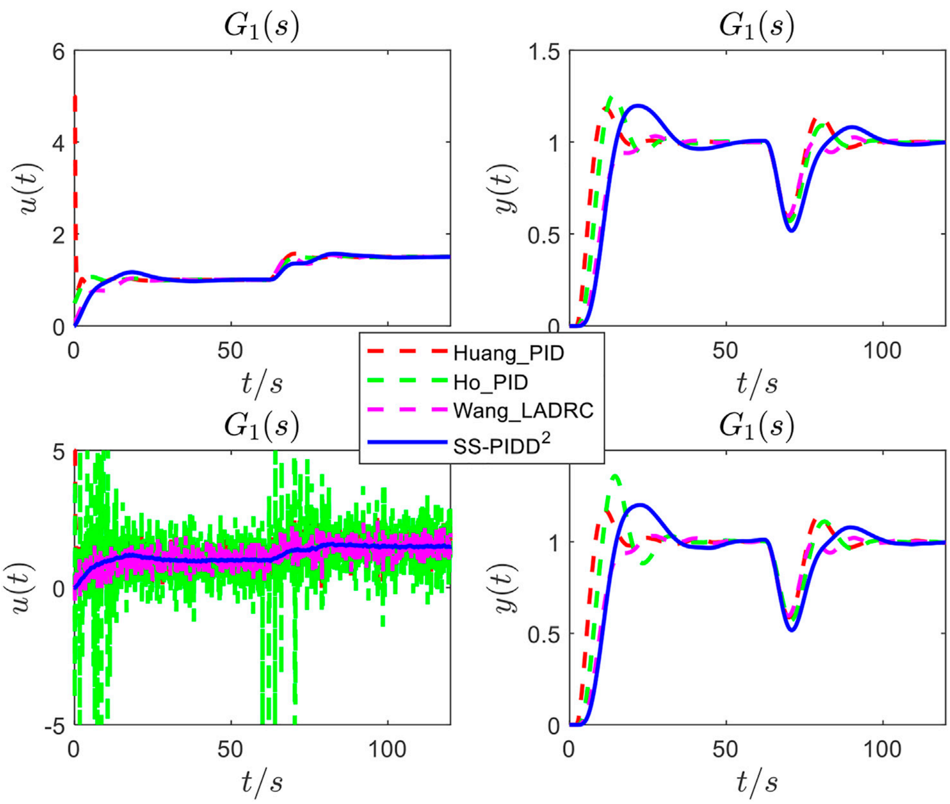

FIGURE 12
Responses of $G_1(s)$: controller output responses without noise (the top left); system output responses without noise (the top right); controller output responses with noise (the bottom left); system output responses with noise (the bottom right).

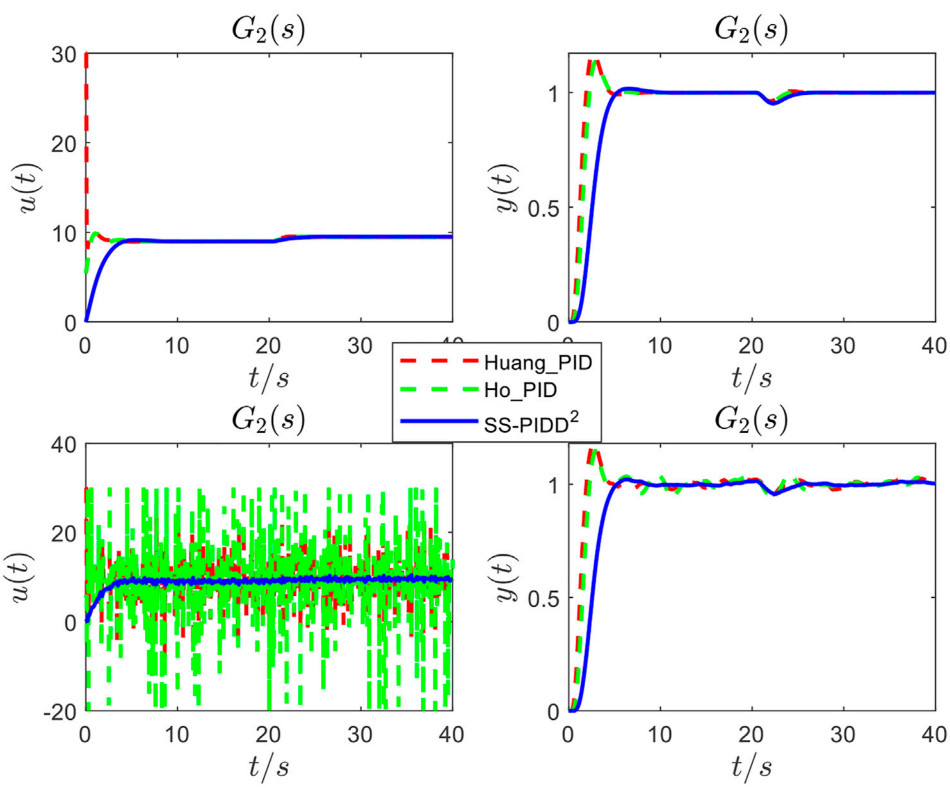

FIGURE 13
Responses of $G_2(s)$: controller output responses without noise (the top left); system output responses without noise (the top right); controller output responses with noise (the bottom left); system output responses with noise (the bottom right).

TABLE 2 Parameters of the SS-$PIDD^2$ and PID controllers for $\xi = 0.4$.

System parameters		Method	Controller parameters				ITSE index	Robustness index	Total variation
			K_p	K_i	K_d	K_{dd}	ITSE	ε	TV
$\xi = 0.4$	$\tau/T = 1$	SS-$PIDD^2$	0.0334	0.2296	0.2665	−0.0375	407.3708	1.9260	8.3491
		Huang_PID	0.4	0.5	0.5		239.4808	2.4527	143.7389
		Ho_PID	0.3334	0.3840	0.3840		245.4935	2.0665	781.3864
	$\tau/T = 2$	SS-$PIDD^2$	0.1313	0.1973	0.1246	0.0626	658.5166	2.1135	9.1303
		Huang_PID	0.2	0.25	0.25		565.4083	2.4028	71.8414
		Ho_PID	0.1601	0.1920	0.1920		618.3568	2.0001	397.009
	$\tau/T = 3$	SS-$PIDD^2$	0.2648	0.1698	0.1180	0.0613	989.0638	2.2598	16.3053
		Huang_PID	0.1333	0.1667	0.1667		1.064e+03	2.3872	78.2354
		Ho_PID	0.1053	0.1280	0.1280		1.238e+03	2.0061	445.3830
	$\tau/T = 4$	SS-$PIDD^2$	0.3551	0.1556	0.1958	0.0944	1.2933+03	2.4294	24.6455
		Huang_PID	0.1000	0.1250	0.1250		1.668e+03	2.3785	58.6884
		Ho_PID	0.0784	0.0960	0.0960		1.996e+03	2.0083	336.0283

TABLE 3 Parameters of the SS-$PIDD^2$ and PID controllers for $\xi = 0.6$.

System parameters		Method	Controller parameters				ITSE index	Robustness index	Total variation
			K_p	K_i	K_d	K_{dd}	ITSE	ε	TV
$\xi = 0.6$	$\tau/T = 1$	SS-$PIDD^2$	0.2490	0.2701	0.2346	−0.0481	291.8792	1.8584	8.4226
		Huang_PID	0.6	0.5	0.5		170.1537	2.4198	233.3799
		Ho_PID	0.4870	0.3840	0.3840		195.1879	2.0467	782.5537
	$\tau/T = 2$	SS-$PIDD^2$	0.3113	0.2210	0.2060	0.0282	508.1148	2.0735	11.7401
		Huang_PID	0.3	.25	0.25		483.9737	2.3854	116.6628
		Ho_PID	0.2369	0.1920	0.1920		567.9483	2.0036	413.0732
	$\tau/T = 3$	SS-$PIDD^2$	0.3747	0.1871	0.2141	0.0596	858.4619	2.3263	23.2255
		Huang_PID	0.2	0.1667	0.1667		1.009e+03	2.3758	126.8926
		Ho_PID	0.1565	0.1280	0.1280		1.206e+03	2.0071	430.8983
	$\tau/T = 4$	SS-$PIDD^2$	0.4140	0.1632	0.2244	0.0903	1.212e+03	2.5511	26.6605
		Huang_PID	0.1500	0.1250	0.1250		1.611e+03	2.3700	90.2657
		Ho_PID	0.1168	0.0960	0.0960		1.971e+03	2.0087	283.7364

where $\bar{\tau}$ varies from 2.5 to 5 with an appropriate step. A set of parameters of SS-$PIDD^2$ K_p, K_i, K_d, K_{dd}, and ω_o can be obtained through the process in Figure 4. The fitting curves of parameters of SS-$PIDD^2$ are shown in Figures 7, 9.

The corresponding function expressions are given in Eq. 45:

$$\begin{aligned} \bar{K}_p &= -0.0452\bar{\tau}^2 + 0.5190\bar{\tau} - 0.9770,\\ \bar{K}_i &= 0.0016\bar{\tau}^2 - 0.0111\bar{\tau} + 0.2372,\\ \bar{K}_d &= -0.0059\bar{\tau}^2 + 0.2437\bar{\tau} - 0.7264,\\ \bar{K}_{dd} &= 0.0878\bar{\tau}^2 - 0.5952\bar{\tau} + 1.0306,\\ \bar{\omega}_o &= -0.0800\bar{\tau}^2 + 0.4963\bar{\tau} + 3.8536. \end{aligned} \tag{45}$$

Similar to Eq. 44, we can obtain the following:

$$\begin{aligned} A_1 &= -0.0909\xi^2 + 0.1645\xi - 0.07444,\\ A_2 &= 1.405\xi^2 - 2.175\xi + 0.8978,\\ A_3 &= -3.166\xi^2 + 5.363\xi - 1.923,\\ B_1 &= 0.02167\xi^2 - 0.01522\xi + 0.003777,\\ B_2 &= -0.09188\xi^2 - 0.001259\xi - 0.007188,\\ B_3 &= 0.3004\xi^2 + 0.007393\xi + 0.1756,\\ C_1 &= 7.843e - 09\xi^{-6.822} - 0.006375,\\ C_2 &= 0.6736\xi^2 - 1.011\xi + 0.419,\\ C_3 &= 2.95\xi^2 + 4.443\xi - 1.497,\\ D_1 &= 0.04845\xi^{-0.7432} - 0.07248,\\ D_2 &= -0.286\xi^{-0.8213} + 0.4774,\\ D_3 &= 0.4976\xi^{-0.8112} - 0.8055,\\ E_1 &= -0.02299\xi^{-1.035} + 0.04166,\\ E_2 &= 0.1223\xi^{-1.143} - 0.2734,\\ E_3 &= -0.1418\xi^{-1.264} + 4.938. \end{aligned} \tag{46}$$

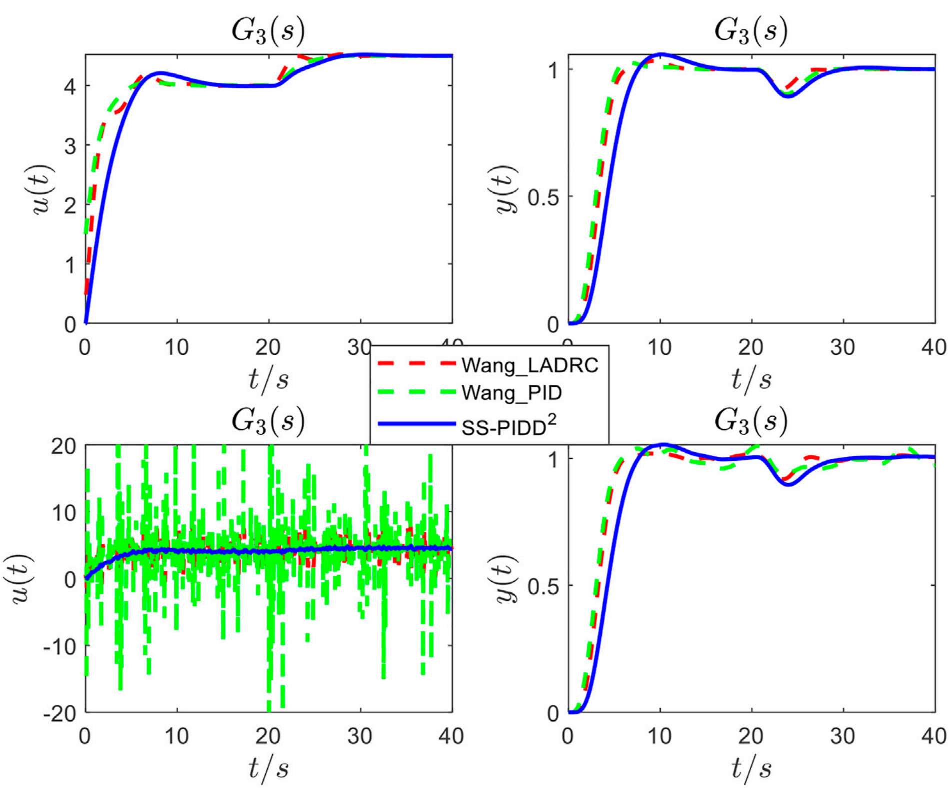

FIGURE 14
Responses of $G_3(s)$: controller output responses without noise (the top left); system output responses without noise (the top right); controller output responses with noise (the bottom left); system output responses with noise (the bottom right).

TABLE 4 Parameters of the SS-*PIDD*^{2} and PID controllers for (50)–(52).

System parameters				Method	Controller parameters					ITSE index	Robustness index	Total variation
	ξ	τ	T		K_p	K_i	K_d	K_{dd}	ω_o	ITSE	ε	TV
G1	0.4154	2.3000	3.2024	SS-*PIDD*^{2}	0.0364	0.0769	1.0554	−0.928	1.4554	1.99e+03	2.4288	0.6661
				Huang_PID	0.5784	0.2174	2.2294			1.14e+03	3.0657	0.7360
				Ho_PID	0.4950	0.1669	1.7121			1.21e+03	2.4928	0.5826
				Wang_LADRC					4.7154	929.7305	4.01	1.0383
G2	0.5704	0.5230	0.6321	SS-*PIDD*^{2}	1.9936	4.1681	1.5514	−0.260	7.3497	1.0107	1.8594	0.5117
				Huang_PID	6.5994	9.1520	3.6568			0.3753	2.4264	0.5814
				Ho_PID	5.4345	7.0282	2.8082			0.4661	2.0704	0.5084
G3	0.4911	0.8370	1.1207	SS-*PIDD*^{2}	0.5322	1.0544	1.4873	−0.459	4.1540	15.5827	1.9197	0.5407
				Wang_LADRC					13.323	4.5426	2.7579	0.6918
				Wang_PID	1.5030	1.3660	1.7150			10.3836	1.7707	0.5069

When $\xi = 0.1; 0.3; 0.4; 0.5; 0.6; 0.7$, the corresponding fitting curves of K_p, K_i, K_d, K_{dd}, ω_o, and ξ are obtained, as shown in Figures 8, 10.

In practice, the relationship between $\bar{K}_p$, $\bar{K}_i$, $\bar{K}_d$, $\bar{K}_{dd}$, and $\bar{\omega}_o$ of SS-$PIDD^2$ for the normalized SOPDT model in Eq. 41 and K_p, K_i, K_d, K_{dd}, and ω_o of SS-$PIDD^2$ for the general SOPDT model in Eq. 26is described in the following (Zhang et al., 2019):

$$K_p = \frac{\bar{K}_p}{k},\quad K_i = \frac{\bar{K}_i}{Tk},\quad K_d = \frac{\bar{K}_d T}{k},\quad K_{dd} = \frac{\bar{K}_{dd} T^2}{k},\quad \omega_o = \frac{\bar{\omega}_o}{T}. \quad (47)$$

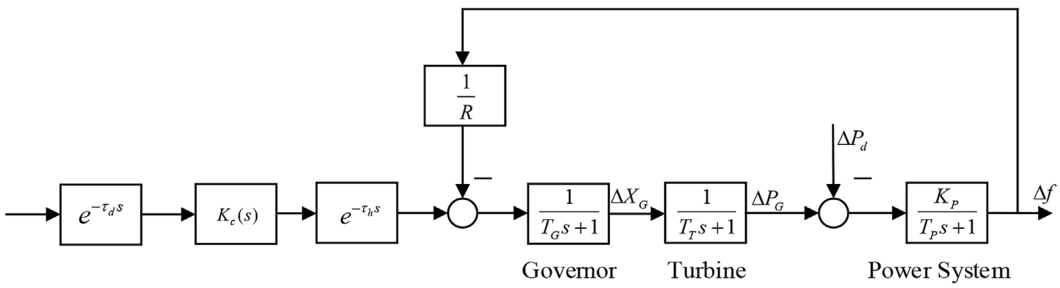

FIGURE 15
Transfer function model of the load frequency control system.

As a result, combining Eqs 43–47, we can obtain the following tuning formula of SS-$PIDD^2$ for the SOPDT system:

$$
\begin{aligned}
K_p &= \frac{\left(0.3\xi^2 - 0.4434\xi + 0.1691\right)\tau^2}{kT^2} + \frac{\left(-1.102\xi^2 + 1.354\xi - 0.3866\right)\tau}{kT} + \frac{0.7656\xi^2 + 0.2038\xi - 0.189}{k},\\
K_i &= \frac{\left(0.02727\xi^2 - 0.01403\xi + 0.01164\right)\tau^2}{kT^3} + \frac{\left(-0.1443\xi^2 + 0.02041\xi - 0.04854\right)\tau}{kT^2} + \frac{0.313\xi + 0.1575}{kT},\\
K_d &= \frac{\left(-0.2909\xi^2 + 0.06036\xi + 0.1023\right)\tau^2}{kT} + \frac{(1.258\xi - 0.8848)\tau}{k} + \frac{(-1.187\xi + 1.043)T}{k},\\
K_{dd} &= \frac{\left(-0.3103\xi^2 + 0.4958\xi - 0.2201\right)\tau^2}{k} + \frac{\left(0.8436\xi^2 - 1.519\xi + 0.787\right)\tau T}{k} + \frac{\left(-0.5418\xi^2 + 0.9786\xi - 0.5852\right)T^2}{k},\\
\omega_o &= \frac{\left(0.4148\xi^2 - 0.5456\xi + 0.205\right)\tau^2}{T^3} + \frac{\left(-3.695\xi^{-0.04876} + 3.626\right)\tau}{T^2} + \frac{-56.83\xi^{0.00182} + 61.54}{T}.
\end{aligned}
\tag{48}
$$

Similarly, using the same process, we can obtain the tuning formula when $\tau/T > 2.5$ as follows:

$$
\begin{aligned}
K_p &= \frac{\left(-0.0909\xi^2 + 0.1645\xi - 0.07444\right)\tau^2}{kT^2} + \frac{\left(1.405\xi^2 - 2.175\xi + 0.8978\right)\tau}{kT} + \frac{-3.166\xi^2 + 5.363\xi - 1.923}{k},\\
K_i &= \frac{\left(0.02167\xi^2 - 0.01522\xi + 0.003777\right)\tau^2}{kT^3} + \frac{\left(-0.09188\xi^2 - 0.001259\xi - 0.007188\right)\tau}{kT^2} + \frac{0.3004\xi^2 + 0.007393\xi + 0.1756}{kT},\\
K_d &= \frac{\left(7.843e-09\xi^{-6.822} - 0.006375\right)\tau^2}{kT} + \frac{\left(0.6736\xi^2 - 1.011\xi + 0.419\right)\tau}{k} + \frac{\left(-2.95\xi^2 + 4.443\xi - 1.497\right)T}{k},\\
K_{dd} &= \frac{\left(0.04845\xi^{-0.7432} - 0.07248\right)\tau^2}{k} + \frac{\left(-0.286\xi^{-0.8213} + 0.4774\right)\tau T}{k} + \frac{\left(0.4976\xi^{-0.8112} - 0.8055\right)T^2}{k},\\
\omega_o &= \frac{\left(-0.02299\xi^{-1.035} + 0.04166\right)\tau^2}{T^3} + \frac{\left(0.1223\xi^{-1.143} - 0.2734\right)\tau}{T^2} + \frac{-0.1418\xi^{-1.264} + 4.938}{T}..
\end{aligned}
\tag{49}
$$

4 Simulation and analyses

This section demonstrates the tuning formula for several examples. In every simulation example, a different control effect has been analyzed and compared with existing methods.

4.1 Simple simulation examples

Simple second-order oscillatory plants with damping ratios ($\xi = 0.2, \xi = 0.4, \xi = 0.6$) and delay time ($T = 1, \tau/T = 1, 2, 3, 4$) are shown in Figures 7–11 (the figures show controller outputs $u(t)$ within the appropriate range; otherwise, $u(t)$ for the disturbance response will be too small to be visible in the figure). The parameters and indexes ($(ITSE = \int_0^\infty te^2(t)dt$; $\varepsilon{:} = \sup_\omega(\|S\|_\infty + \|T\|_\infty)$; $(TV = \sum_1^\infty |u_{i+1}(t) - u_i(t)|)$) are shown in Tables 1–3. The responses for a step reference signal (the amplitude is 1) at $t = 0s$ and a step input disturbance signal (the amplitude is .5) are added to these systems at an appropriate time to test the disturbance rejection performance and robustness. Moreover, suppose there is a white noise signal with a variance of 0.001 added to the output of the plant to test the performance of measurement noise attenuation. From Figures 7–10, we can see that the output responses of the system with $\xi = 0.2; 0.4$ show large oscillations, which is because the poles of the system are close to the imaginary axis. The responses of the system with $\xi = 0.6$ are shown in Figure 11. Compared with the PID controller, the SS-$PIDD^2$ controller has a faster tracking and disturbance rejection response. Moreover, the SS-$PIDD^2$ controller has smaller overshooting and fluctuation than the PID controller. In particular, after adding noise, the SS-$PIDD^2$ controller output response is significantly better than the other two PID methods. Combining figures and tables, we can see that the tuning in Eqs 48, 49 can achieve a better response. Therefore, we can conclude that the proposed formula of SS-$PIDD^2$ has a better control effect for the SOPDT system.

Remark: 1) Robustness is the property that a control system maintains for some other performance under certain (structure and size) parameter perturbations.

$$
M_s = \|S\|_\infty = \max_\omega \left|\frac{1}{1 + L(j\omega)}\right|,
$$

$$
M_t = \|T\|_\infty = \max_\omega \left|\frac{L(j\omega)}{1 + L(j\omega)}\right|,
$$

$$
\varepsilon{:} = \sup_\omega\left(\|S\|_\infty + \|T\|_\infty\right),
$$

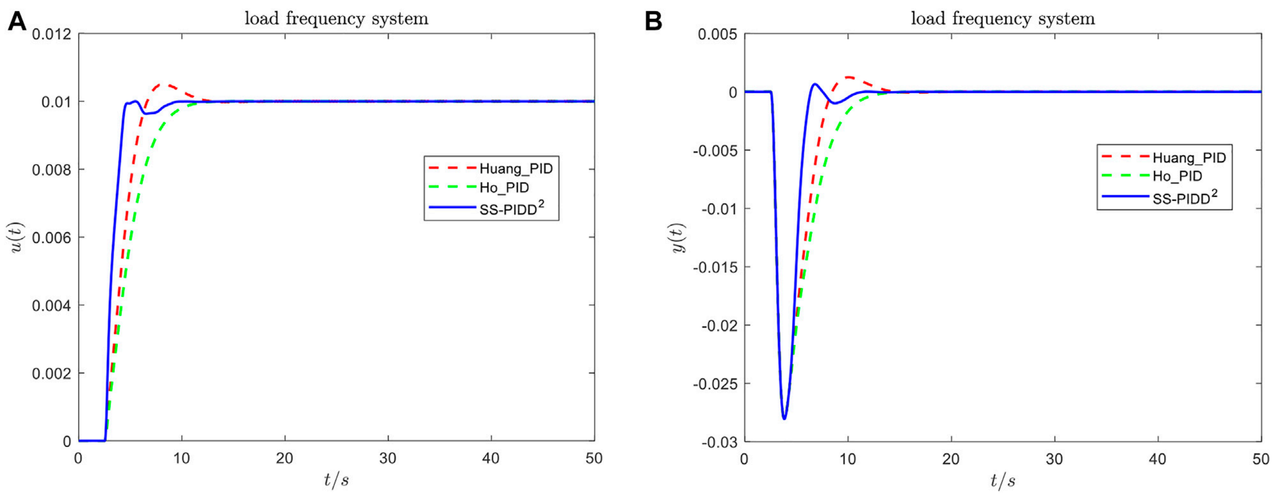

FIGURE 16
System responses under different controllers: **(A)** controller output responses and **(B)** system output responses.

where $L(s)$ is the open-loop transfer function of the system, M_s and M_t are maximum sensitivities, $S(s)$ and $T(s)$ are sensitivity functions, and ε represents the robustness of the system.

2) ITSE is the integral of the time squared error. $ITSE = \int_0^{\infty} te^2(t)dt$. $e(t) = r(t) - y(t)$ is the difference between the reference input signal and output signal of the system.

3) TV is the total variation in the output of the controller. $TV = \sum_1^{\infty}|u_{i+1}(t) - u_i(t)|$.

4.2 Complex simulation examples

In this subsection, we use three relatively complex oscillatory plants (G_1 (Huang et al., 2005), G_2, and G_3 (Wang et al., 1999)) to verify the applicability of the proposed Eqs 48 and 49. Dynamic responses of plants are given in Figures 12–14. The controller parameters, systems parameters, and controller performance index are shown in Table 4. It is shown that SS-$PIDD^2$ and PID have similar disturbance rejection responses; SS-$PIDD^2$ has a smaller overshoot in the set-point for G_1 and set-point tracking responses without the overshoot for G_2 and G_3.Additionally, the influence of the measurement noise on SS-$PIDD^2$ is smaller than PID. Significantly, SS-$PIDD^2$ does not have a satisfactory disturbance rejection performance, compared to the linear active disturbance rejection controller (LADRC) for G_3 but has a smaller robustness and TV than LADRC. Generally speaking, the proposed tuning approach has a better control effort and can trade-off between the performance, robustness, and attenuation of the measurement noise.

$$G_1(s) = \frac{1}{(9s^2 + 2.4s + 1)(s + 1)}e^{-2s}, \tag{50}$$

$$G_2(s) = \frac{1}{(s^2 + 2s + 3)(s + 3)}e^{-0.3s}, \tag{51}$$

$$G_3(s) = \frac{1}{(s^2 + s + 1)(s + 2)^2}e^{-0.1s}. \tag{52}$$

4.3 Practical system simulations

Consider the load frequency control system as a typical oscillatory SOPDT system. Additionally, the system's uncertainty and control complexity will rise due to communication delays. Therefore, the proposed SS-$PIDD^2$ controller is applied to the LFC system with communication delays in this section to test its effectiveness.

To illustrate the issue, we take the one-area non-reheat system as an example (Fu and Tan, 2018). The transfer function model of the LFC system is shown in Figure 15. The transfer function of each part is as follows:

$$G_g(s) = \frac{1}{0.08s + 1}, G_t(s) = \frac{1}{0.3s + 1}, G_p(s) = \frac{120}{20s + 1} \tag{53}$$

and

$$R = 2.4, \tau_d + \tau_h = 1.5. \tag{54}$$

The system parameters are as follows (Fu and Tan, 2018):

$$k = 2.3568, \xi = 0.4665, T = 0.3700, \tau = 1.5\,. \tag{55}$$

Suppose there is a disturbance of $\Delta P_d = 0.01pu$ added to the output of the controller. From Figure 16, we can conclude that the proposed controller has a faster response speed and better disturbance rejection performance.

5 Conclusion

The purpose of this paper was to provide a tuning formula of the $PIDD^2$ controller for oscillatory systems with time delays. The ideal $PIDD^2$ controller was implemented *via* the state-space form, which takes a cascaded integral model to estimate the output of the controlled plant and its derivatives; accordingly, it retains the plant-independence property of the traditional PID. A total of two state-space $PIDD^2$ tuning formulas were attained for SOPDT systems with time delays, and the parameters of $PIDD^2$ can be determined by approximating an IMC controller. The proposed formulas are applied to a wide range of plants. In addition, further simulation analysis of $PIDD^2$ was used to test the effectiveness of the proposed tuning formula. Compared with the PID controller, the state-space $PIDD^2$ controller has roll-offs at high frequencies; thus, it is more insensitive to measurement noises.

The empirical findings in this study provide a new understanding of $PIDD^2$ controllers. Future research will be devoted to the control of $PIDD^2$ oscillatory systems with zeros.

Data availability statement

The raw data supporting the conclusion of this article will be made available by the authors, without undue reservation.

Author contributions

HX, HG, and TW contributed to the conceptualization and methodology. HX wrote the first draft of the manuscript. All authors contributed to manuscript revision and read and approved the submitted version.

Conflict of interest

The authors declare that the research was conducted in the absence of any commercial or financial relationships that could be construed as a potential conflict of interest.

Publisher's note

All claims expressed in this article are solely those of the authors and do not necessarily represent those of their affiliated organizations, or those of the publisher, the editors, and the reviewers. Any product that may be evaluated in this article, or claim that may be made by its manufacturer, is not guaranteed or endorsed by the publisher.

References

Basilio, J. C., and Matos, S. (2002). Design of PI and PID controllers with transient performance specification. *IEEE Trans. Educ.* 45, 364–370. doi:10.1109/te.2002.804399

Borase, R. P., Maghade, D. K., Sondkar, S. Y., and Pawar, S. N. (2021). A review of PID control, tuning methods and applications. *Int. J. Dynam. Control* 9, 818–827. doi:10.1007/s40435-020-00665-4

Chan, Y. F., Moallem, M., and Wang, W. (2007). Design and implementation of modular FPGA-based PID controllers. *IEEE Trans. Ind. Electron.* 54, 1898–1906. doi:10.1109/tie.2007.898283

Chao, C.-T., Sutarna, N., Chiou, J.-S., and Wang, C.-J. (2019). An optimal fuzzy PID controller design based on conventional PID control and nonlinear factors. *Appl. Sci.* 9, 1224. doi:10.3390/app9061224

Chatterjee, S., Dalel, M. A., and Palavalasa, M., 2019. "Design of PID plus second order derivative controller for automatic voltage regulator using whale optimizatio algorithm," in 2019 3rd International Conference on Recent Developments in Control, Automation & Power Engineering (RDCAPE), NOIDA, India, 10-11 October 2019 (IEEE), 574–579.Presented at the 2019 3rd International Conference on Recent Developments in Control, Automation & Power Engineering (RDCAPE).

Chevalier, A., Francis, C., Copot, C., Ionescu, C. M., and De Keyser, R. (2019). Fractional-order PID design: Towards transition from state-of-art to state-of-use. *ISA Trans.* 84, 178–186. doi:10.1016/j.isatra.2018.09.017

Farooq, Z., Rahman, A., and Lone, S. A. (2021). "Fuzzy and MBO optimized load frequency control of hybrid power system," in 2021 IEEE 18th India Council International Conference (INDICON). Presented at the 2021 IEEE 18th India Council International Conference (INDICON), Guwahati, India, 19-21 December 2021 (IEEE), 1–6.

Fu, C., and Tan, W. (2018). Decentralised load frequency control for power systems with communication delays via active disturbance rejection. *IET Generation, Transm. Distribution* 12, 1397–1403. doi:10.1049/iet-gtd.2017.0852

Gao, Z. (2003). "Scaling and bandwidth-parameterization based controller tuning," in Proceedings of the 2003 American Control Conference, 2003, Denver, CO, USA, 04-06 June 2003 (IEEE), 4989–4996. Presented at the 2003 American Control Conference.

Garpinger, O., Hägglund, T., and Åström, K. J. (2014). Performance and robustness trade-offs in PID control. *J. Process Control* 24, 568–577. doi:10.1016/j.jprocont.2014.02.020

Gundes, A. N., and Ozguler, A. B. (2007). PID stabilization of MIMO plants. *IEEE Trans. Autom. Contr.* 52, 1502–1508. doi:10.1109/tac.2007.902763

Halikias, G. D., and Zolotas, A. C. (1999). Optimal design of PID controllers using the QFT method. *IEE Proc. - Control Theory Appl.* 146, 585–589. doi:10.1049/ip-cta:19990746

Horn, I. G., Arulandu, J. R., Gombas, C. J., VanAntwerp, J. G., and Braatz, R. D. (1996). Improved filter design in internal model control. *Ind. Eng. Chem. Res.* 35, 3437–3441. doi:10.1021/ie9602872

Huang, H.-P., Jeng, J.-C., and Luo, K.-Y. (2005). Auto-tune system using single-run relay feedback test and model-based controller design. *J. Process Control* 15, 713–727. doi:10.1016/j.jprocont.2004.11.004

Huang, H.-P., Lee, M.-W., and Chen, C.-L. (2000). Inverse-based design for a modified PID controller. *J. Chin. Inst. Chem. Eng.* 31, 225–236.

Jin, Z., Chen, J., Sheng, Y., and Liu, X. (2017). Neural network based adaptive fuzzy PID-type sliding mode attitude control for a reentry vehicle. *Int. J. Control Autom. Syst.* 15, 404–415. doi:10.1007/s12555-015-0181-1

kalyan, C. N. S., and Suresh, C. V. (2021). "PIDD controller for AGC of nonlinear system with PEV integration and AC-DC links," in 2021 International Conference on Sustainable Energy and Future Electric Transportation (SEFET), Hyderabad, India, 21-23 January 2021 (IEEE), 1–6. Presented at the 2021 International Conference on Sustainable Energy and Future Electric Transportation (SEFET).

Kalyan, C. N. S. (2021). "UPFC and SMES based coordinated control strategy for simultaneous frequency and voltage stability of an interconnected power system," in 2021 1st International Conference on Power Electronics and Energy (ICPEE), Bhubaneswar, India, 02-03 January 2021 (IEEE), 1–6. Presented at the 2021 1st International Conference on Power Electronics and Energy (ICPEE).

Kim, M., and Lee, S.-U. (2021). PID with a switching action controller for nonlinear systems of second-order controller canonical form. *Int. J. Control Autom. Syst.* 19, 2343–2356. doi:10.1007/s12555-020-0346-4

Koley, I., Sarkar, B., Datta, A., and Panda, G. K. (2020). "Load frequency control of a wind energy integrated multiarea power system with CSA tuned PIDD controller," in 2020 IEEE First International Conference on Smart Technologies for Power, Energy and Control (STPEC), Nagpur, India, 25-26 September 2020 (IEEE), 1–6. Presented at the 2020 IEEE First International Conference on Smart Technologies for Power, Energy and Control (STPEC).

Kurokawa, R., Sato, T., Vilanova, R., and Konishi, Y. (2020). Design of optimal PID control with a sensitivity function for resonance phenomenon-involved second-order plus dead-time system. *J. Frankl. Inst.* 357, 4187–4211. doi:10.1016/j.jfranklin.2020.03.015

Lee, Y., Park, S., Lee, M., and Brosilow, C. (1998). PID controller tuning for desired closed-loop responses for SI/SO systems. *AIChE J.* 44, 106–115. doi:10.1002/aic.690440112

Memon, F., and Shao, C. (2020). An optimal approach to online tuning method for PID type iterative learning control. *Int. J. Control Autom. Syst.* 18, 1926–1935. doi:10.1007/s12555-018-0840-0

Memon, F., and Shao, C. (2021). Robust optimal PID type ILC for linear batch process. *Int. J. Control Autom. Syst.* 19, 777–787. doi:10.1007/s12555-019-1033-1

Mohanty, B. (2020). Hybrid flower pollination and pattern search algorithm optimized sliding mode controller for deregulated AGC system. *J. Ambient. Intell. Hum. Comput.* 11, 763–776. doi:10.1007/s12652-019-01348-5

Mohanty, B. (2018). Performance analysis of moth flame optimization algorithm for AGC system. *Int. J. Model. Simul.* 39 (1), 1–15. 16. doi:10.1080/02286203.2018.1476799

Mokeddem, D., and Mirjalili, S. (2020). Improved Whale Optimization Algorithm applied to design PID plus second-order derivative controller for automatic voltage regulator system. *J. Chin. Inst. Eng.* 43, 541–552. doi:10.1080/02533839.2020.1771205

Oliveira, P. B. M., and Vrančić, D. (2012). Underdamped second-order systems overshoot control. *IFAC Proc. Vol.* 45, 518–523. doi:10.3182/20120328-3-it-3014.00088

Pan, T., Li, S., and Cai, W.-J. (2007). Lazy learning-based online identification and adaptive PID control: A case study for cstr process. *Ind. Eng. Chem. Res.* 46, 472–480. doi:10.1021/ie0608713

Radke, F., and Isermannt, R. (1987). *A parameter-adaptive PID-controller with stepwise parameter optimization 9*. Elsevier.

Shamsuzzoha, M., and Lee, M. (2008). Analytical design of enhanced PID filter controller for integrating and first order unstable processes with time delayfilter controller for integrating and first order unstable processes with time delay. *Chem. Eng. Sci.* 15, 2717–2731. doi:10.1016/j.ces.2008.02.028

Shamsuzzoha, M., and Lee, M. (2007). IMC–PID controller design for improved disturbance rejection of time-delayed processes. *Ind. Eng. Chem. Res.* 46, 2077–2091. doi:10.1021/ie0612360

Simanenkov, A. L., Rozhkov, S. A., and Borisova, V. A. (2017). "An algorithm of optimal settings for PIDD 2 D 3 -controllers in ship power plant," in 2017 IEEE 37th International Conference on Electronics and Nanotechnology (ELNANO), Kyiv, Ukraine (IEEE), 152–155. Presented at the 2017 IEEE 37th International Conference on Electronics and Nanotechnology (ELNANO).

Skogestad, S., and Grimholt, C. (2012). "The SIMC method for smooth PID controller tuning," in *PID control in the third millennium, advances in industrial control*. Editors R. Vilanova, and A. Visioli (London: Springer London), 147–175.

Sonkar, P., and Rahi, O. P. (2016). "Unified tuning of PID-derivative filter load frequency controller for two area interconnected system including wind power plant," in 2016 IEEE Uttar Pradesh Section International Conference on Electrical, Computer and Electronics Engineering (UPCON), Varanasi, India, 09-11 December 2016 (IEEE), 388–393. Presented at the 2016 IEEE Uttar Pradesh Section International Conference on Electrical, Computer and Electronics Engineering (UPCON).

Tan, W., and Fu, C. (2015). Linear active disturbance rejection control: Analysis and tuning via IMC. *IEEE Trans. Ind. Electron.* 63, 2350–2359. doi:10.1109/tie.2015.2505668

Tzafestas, S., and Papanikolopoulos, N. P. (1990). Incremental fuzzy expert PID control. *IEEE Trans. Ind. Electron.* 37, 365–371. doi:10.1109/41.103431

Wang, Q-G., Lee, T-H., Fung, H-W., Bi, Q., and Zhang, Y. (1999). PID tuning for improved performance. *IEEE Trans. Contr. Syst. Technol.* 7, 457–465. doi:10.1109/87.772161

Wang, Y., Tan, W., Cui, W., Han, W., and Guo, Q. (2021). Linear active disturbance rejection control for oscillatory systems with large time-delays. *J. Frankl. Inst.* 358, 6240–6260. doi:10.1016/j.jfranklin.2021.06.016

Weng, K. H., Chang, C. H., and Zhou, J. (1997). Self-tuning PID control of a plant with under-damped response with specifications on gain and phase margins. *IEEE Trans. Contr. Syst. Technol.* 5, 446–452. doi:10.1109/87.595926

Zhang, B., Tan, W., and Li, J. (2019). Tuning of linear active disturbance rejection controller with robustness specification. *ISA Trans.* 10, 237–246. doi:10.1016/j.isatra.2018.10.018

Zhao, C., Xue, D., and Chen, Y. Q. (2005). "A fractional order PID tuning algorithm for a class of fractional order plants," in IEEE International Conference Mechatronics and Automation, 2005, Niagara Falls, ON, Canada (IEEE), 216–221. Presented at the 2005 IEEE International Conference on Mechatronics and Automation.